Received: 21 November 2019 | Accepted: 28 April 2020

DOI: 10.1002/mrd.23348

Molecular Reproduction & Development

RESEARCH ARTICLE

Whole-body heat exposure causes developmental stage-specific apoptosis of male germ cells

Jungbin Yoon | Kunsoo Rhee

Department of Biological Sciences, Seoul National University, Seoul, Korea

Correspondence
Kunsoo Rhee, Department of Biological Sciences, Seoul National University, Seoul 08826, Korea.
Email: rheek@snu.ac.kr

Funding information
National Research Foundation of Korea, Grant/Award Number: 2019R1A2C2002726

Abstract

Humans are occasionally exposed to extreme environmental heat for a prolonged period of time. Here, we investigated testicular responses to whole-body heat exposure by placing mice in a warm chamber. Among the examined tissues, the testis was found to be most susceptible to heat stress. Heat stress induces direct responses within germ cells, such as eukaryotic initiation factor 2α phosphorylation and stress granule (SG) formation. Prolonged heat stress (42°C for 6 hr) also disturbed tissue organization, such as through blood-testis barrier (BTB) leakage. Germ cell apoptosis was induced by heat stress for 6 hr in a cell type- and developmental stage-specific manner. We previously showed that spermatocytes in the early tubular stages (I–VI) form SGs for protection against heat stress. In the mid-tubular stages (VII–VIII), BTB leakage synergistically enhances the adverse effects of heat stress on pachytene spermatocyte apoptosis. In the late tubular stages (IX–XII), SGs are not formed and severe leakage of the BTB does not occur, resulting in mild apoptosis of late-pachytene spermatocytes near meiosis. Our results revealed that multiple stress responses are involved in germ cell damage resulting from prolonged heat stress (42°C for 6 hr).

KEYWORDS

apoptosis, blood-testis barrier, spermatocyte, thermal stress, whole-body heat

1 | INTRODUCTION

Testes in many mammalian species are extruded outside the body to maintain a temperature 2–3°C below body temperature for optimal spermatogenesis. In other mammals, tested are located within the abdomen but appear to be cooled by special blood vessels, at least in dolphins and seals (Kim, Park, & Rhee, 2013; Pabst, Rommel, McLellan, Williams, & Rowles, 1995). In fact, mouse male germ cells perceive core body temperature as stress (Kim, Cooke, & Rhee, 2012; Zhao et al., 2010). Abnormalities, such as cryptorchidism and varicocele, result in exposure of the testes to raised temperatures and compromised sperm quality, which may lead to a loss of male fertility (Durairajanayagam, Agarwal, & Ong, 2015).

Numerous studies have indicated that high temperatures are deleterious to mammalian spermatogenesis, but the exact mechanisms remain elusive (Hansen, 2009; Houston et al., 2018). Reduced translation activity is one of the initial responses in male germ cells under heat stress. Heat exposure reduces polysome formation and amino acid incorporation into proteins in male germ cells (Cataldo, Mastrangelo, & Kleene, 1997). In fact, the translation initiation complex fails to form, partly because eukaryotic initiation factor 2α (eIF2α) is phosphorylated in male germ cells (Kim et al., 2012;

Abbreviations: BSA, bovine serum albumin; BTB, blood-testis barrier; $CdCl_2$, cadmium chloride; Cdk5, cyclin-dependent kinase 5; DAPI, 4′,6-diamidino-2-phenylindole; Dazl, deleted in azoospermia-like; eIF2α, eukaryotic initiation factor 2α; H&E, hematoxylin & eosin; HSF, heat shock transcription factor; HSP, heat shock protein; PARP, poly ADP ribose polymerase; SG, stress granule; TIA-1, T cell intracellular antigen-1; TUNEL, terminal deoxynucleotidyl transferase dUTP nick end labeling.

Nakamura & Hall, 1980). Heat stress eventually induces apoptotic responses involving nitric oxide synthase and p38 mitogen-activated protein kinase (DeFoor, Kuan, Pinkerton, Sheldon, & Lewis, 2004; Ishikawa, Kondo, Goda, & Fujisawa, 2005).

Protective mechanisms also function to overcome the adverse effects of heat stress on male germ cells. Heat shock proteins (HSPs) are known to play a protective role in preventing heat stress-induced nonspecific aggregation and thermal denaturation of cellular proteins. Heat-inducible HSPs are activated by heat shock transcription factors (HSFs). Heat stress induces the translocation of monomeric HSF1 from the cytoplasm to the nucleus (Baler, Dahl, & Voellmy, 1993), where HSF1 forms trimers for activation and binds to heat shock elements to activate transcription of *HSP* genes in heat-stressed spermatocytes (Dayalan Naidu & Dinkova-Kostova, 2017; Vydra et al., 2006). Another protective mechanism is stress granule (SG) formation. SGs are non-membranous cytoplasmic particles in which translationally inert messenger ribonucleoproteins accumulate in response to stress (Anderson & Kedersha, 2008). We previously reported that SGs are immediately assembled in male germ cells upon acute heat stress (Kim et al., 2012). The suppression of SG formation resulted in the augmentation of apoptosis in male germ cells (Yoon, Park, Hwang, & Rhee, 2017).

The mammalian testis is a complex organ containing both germ cells and somatic cells. Mammalian male germ cells develop within seminiferous tubules in the testis. In mice, the complete spermatogenesis process takes 35 days. Male germ cells develop rhythmically, and consequently, germ cells show a characteristic association in particular stages of spermatogenesis within a given cross-section of a seminiferous tubule. In mice, the seminiferous tubule cycle has been divided into 12 stages, each with a characteristic set of spermatogenic cells in association with one another (Ventela, Ohta, Parvinen, & Nishimune, 2002). Therefore, it is possible to assign a specific stage to the seminiferous tubule cycle and, therefore, to more precisely determine the stage of the cells present (Hogarth & Griswold, 2010). Sertoli cells are somatic cells in the seminiferous tubules that nourish developing male germ cells with signaling molecules and nutrients (Morrow, Mruk, Cheng, & Hess, 2010). Sertoli cells keep the blood-testis barrier (BTB) intact by properly organizing tight junctions, which divide the basal and adluminal compartments within a single seminiferous tubule (Mruk & Cheng, 2015). When the BTB is disrupted, defects in spermatogenesis occur (Alam & Kurohmaru, 2014; Session et al., 2001).

Humans are occasionally exposed to environmental heat for a prolonged period in the workplace or due to an extensive heat wave (Hifumi, Kondo, Shimizu, & Miyake, 2018; Li et al., 2014; Reitman, 2018). In this study, we determined the heat stress-induced responses of the testes after exposing mice to high temperatures (37–42°C) for a prolonged period (6 hr). We hypothesize that tissue organization of the testis may be damaged by prolonged heat exposure (42°C for 6 hr). Male germ cells in disorganized testes may be more vulnerable to heat-induced damage signals, resulting in germ cell apoptosis.

2 | RESULTS

2.1 | Effects of whole-body heat stress on the testis

Our bodies are occasionally exposed to an extreme heat environment. To mimic environmental heat exposure, we placed mice in heat chambers maintained at 25 (control), 32, 37, or 42°C for extended periods up to 6 hr. Next, to assess the organ-specific response to prolonged whole-body heat stress, we examined testis-specific histology compared with other organs with known thermosensitivity (Bazille et al., 2005; Liu et al., 2011; Roberts et al., 2008; Wang et al., 2015). Hematoxylin and eosin (H&E) staining analysis revealed few changes in the histology of the lung, small intestine, and brain tissues after mice were maintained at 42°C for 6 hr (Figure 1a). However, we observed significantly altered overall organization of the testis tissue (Figure 1a). Upon closer examination, apoptotic germ cells with pycnotic nuclei were observed even at 37°C for 6 hr (Figure 1b). Severe heat stress at 42°C was deleterious to testis morphology, resulting in multinucleated giant cells that had been observed under other damaging conditions (Figure 1b; Luo et al., 2013). Since H&E staining showed temperature- and heat exposure time-dependent histological alterations to seminiferous tubules, we decided to investigate more advanced molecular responses to reveal testicular alterations with respect to different exposure times and temperatures.

2.2 | Stress granule formation as transient heat protection

It was previously reported that heat stress induces the specific phosphorylation of eIF2α in male germ cells (Kim et al., 2012; Yoon et al., 2017). We determined eIF2α phosphorylation levels in the testes after prolonged heat stress (37–42°C for 6 hr) and found that eIF2α was immediately phosphorylated after exposing mice to mild heat at 32°C (Figure 2a,b). The eIF2α phosphorylation levels consistently increased thereafter (Figure 2a,b). Poly ADP ribose polymerase (PARP) levels were simultaneeously determined to estimate apoptosis. The cellular PARP levels were not significantly changed by heat stress, while a cleaved PARP band appeared at 2 hr at 37°C and was most prominent at 6 hr at 42°C (Figures 2a,c).

It was previously reported that heat stress induces SG formation in deleted in azoospermia-like (Dazl)-positive spermatocytes (Kim et al., 2012). We used Dazl and T cell intracellular antigen-1 (TIA-1) antibodies to examine SGs in the testes. The results showed immediate SG formation upon exposing mice to severe heat at 42°C, but they quickly dissolved within 2 hr (Figure 2d–f). These results suggest that SG formation is a transient protection mechanism against heat stress.

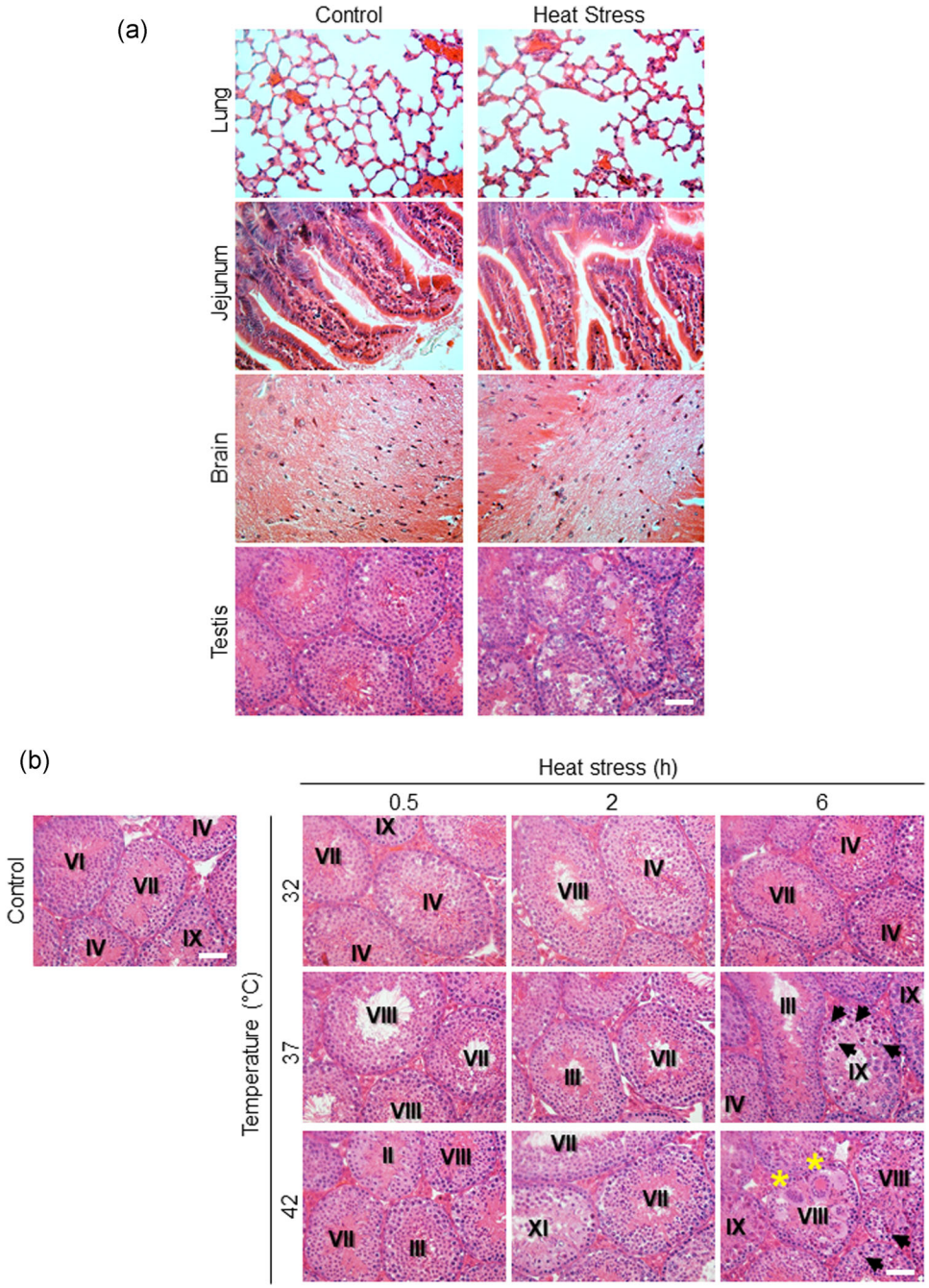

FIGURE 1 Histological analyses of selected mouse tissues under prolonged heat stress. (a) Mice were subjected to prolonged heat stress at 42°C for 6 hr. H&E staining was conducted with the lung, small intestine, brain, and testis tissues. Scale bar = 50 μm. (b) H&E staining of the testes from control and heat-stressed (32, 37, and 42°C) mice are presented. Heat-treated groups were exposed to each temperature setting at given time points (0.5, 2, and 6 hr). Black arrows, germ cells undergoing apoptosis (pycnotic cells). Yellow asterisks, multinucleated giant cells. Scale bar = 50 μm. H&E, hematoxylin & eosin

2.3 | Tubular stage specificity of male germ cell apoptosis under heat stress

We performed terminal deoxynucleotidyl transferase dUTP nick end labeling (TUNEL) assays to determine germ cell apoptosis after heat stress. The results showed that the number of apoptotic germ cells increased after prolonged heat stress (37–42°C for 6 hr; Figure 3a,b). These results are consistent with previous immunoblot results, which displayed a cleaved PARP band after prolonged heat treatments (37–42°C for 6 hr; Figures 2a,c). Furthermore, germ cell apoptosis appeared to be specific to the seminiferous tubule stage. Stages of seminiferous tubules were determined using 4′,6-diamidino-2-phenylindole (DAPI) staining (Meistrich & Hess, 2013). It was found that prolonged heat stress (42°C) for 6 hr increased germ cell

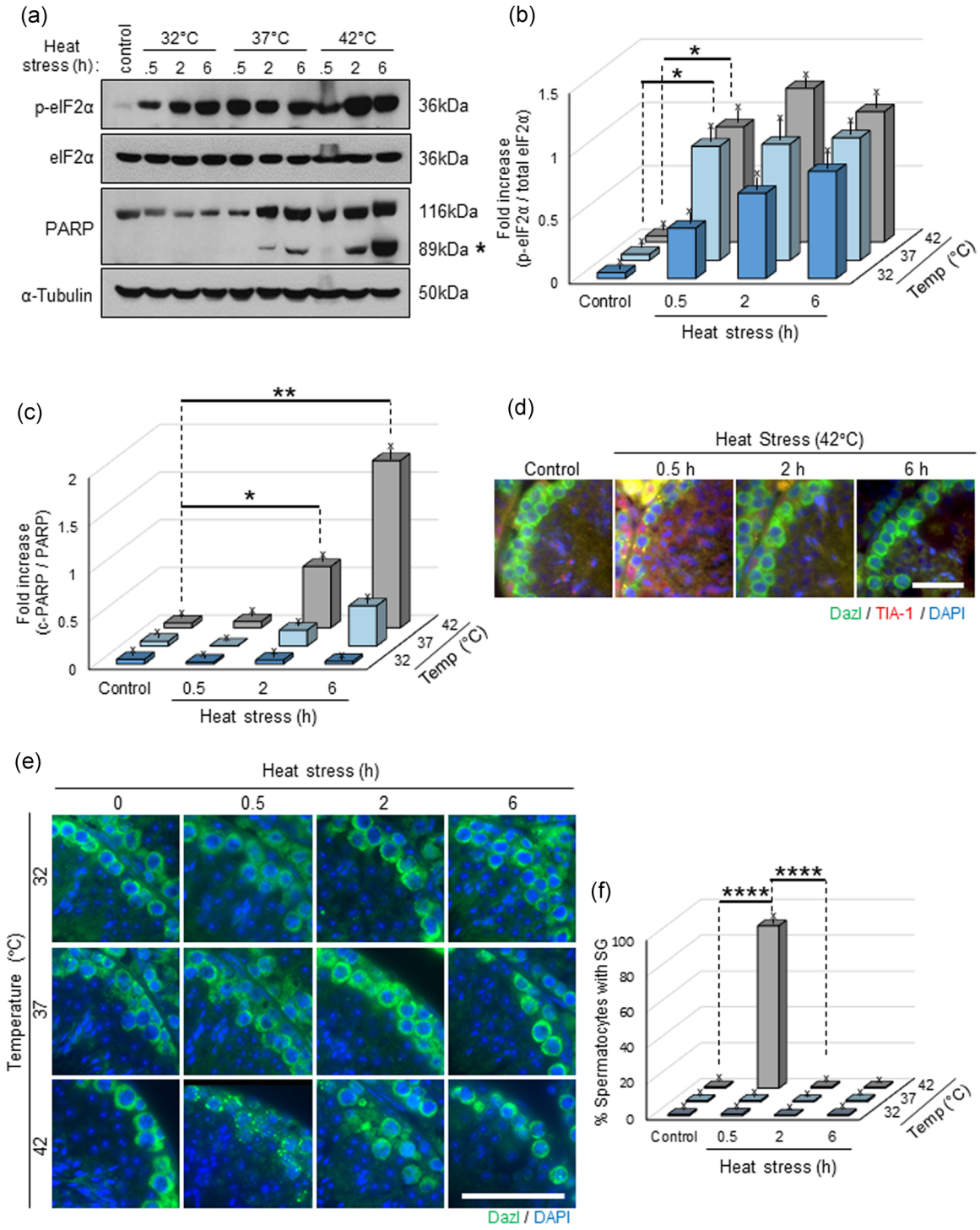

FIGURE 2 Transient formation of SGs in spermatocytes under prolonged heat stress. (a) Mice were subjected to heat stress at 32, 37, and 42°C for the indicated time periods (control, 0.5, 2, and 6 hr). Testes were analyzed by immunoblot using antibodies specific to phospho-eIF2α, eIF2α, PARP, and α-tubulin. Asterisks indicate cleaved PARP (89 kDa). The intensities of phospho-eIF2α (b) and cleaved PARP (c) were determined. (d) SGs were immunostained with Dazl (green), TIA-1 (red), and DAPI (blue). Scale bar = 50 μm. (e) Testes were immunostained with Dazl (green) and TIA-1 (red) antibodies. DNA was stained with DAPI (blue). Scale bar = 50 μm. (f) The proportion of SG-positive spermatocytes was determined. Over 500 spermatocytes per group were analyzed in three mice and were statistically analyzed using one-way ANOVA. The values are the means and *SEM*. ANOVA, analysis of variance; DAPI, 4′,6-diamidino-2-phenylindole; Dazl, deleted in azoospermia-like; eIF2α, eukaryotic initiation factor 2α; PARP, poly ADP ribose polymerase; *SEM*, standard error of mean; SG, stress granule; TIA-1, T cell intracellular antigen-1. $^{*}p < .05$; $^{**}p < .01$; $^{****}p < .0001$

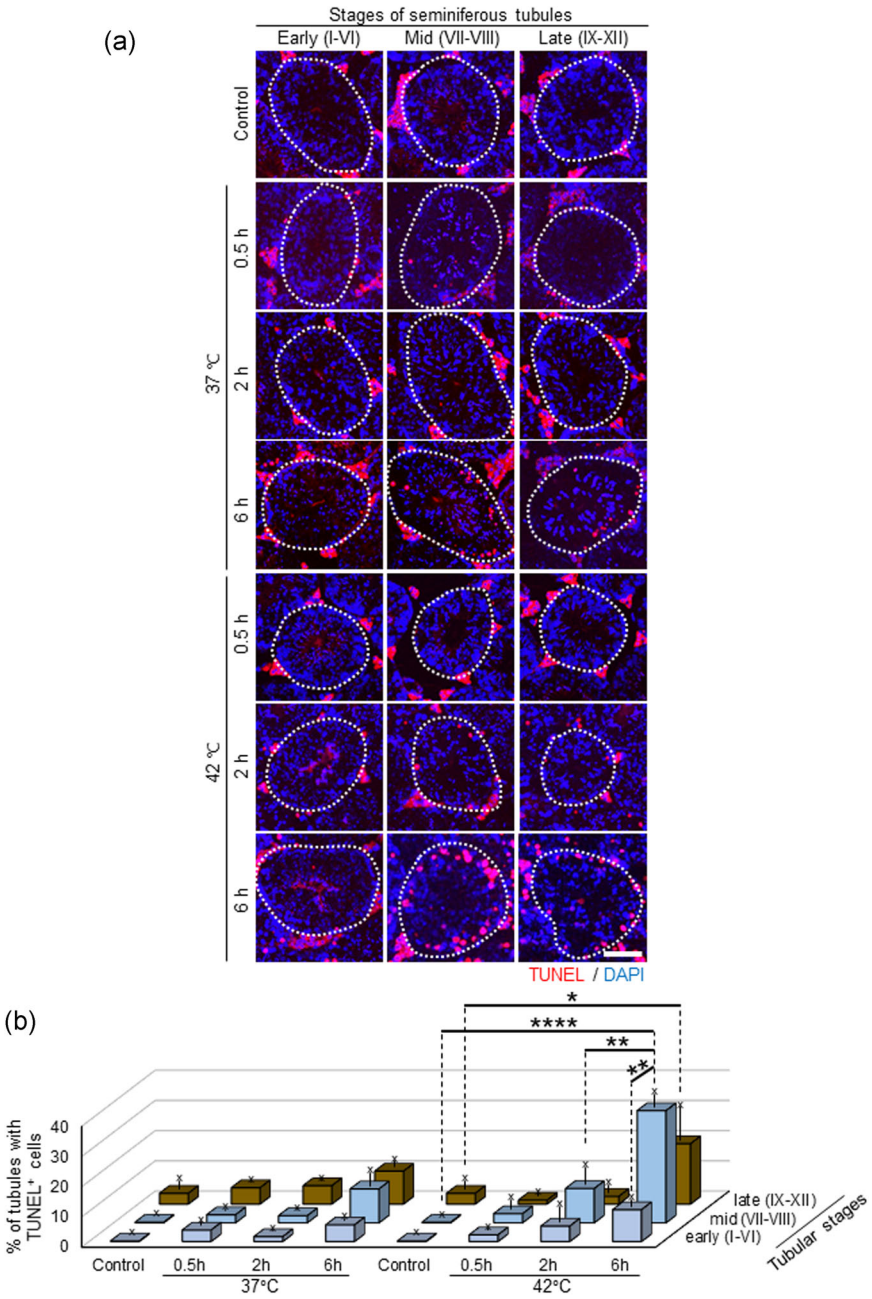

FIGURE 3 Tubular stage specificity of germ cell apoptosis upon prolonged heat stress. (a) Testis sections from the heat-stressed mice were subjected to TUNEL assays (red). DNA was stained with DAPI (blue). Seminiferous tubules were grouped into early (I–VI), mid (VII–VIII), and late (IX–XII) stages. Dashed lines indicate the basal membrane of the seminiferous tubules. Scale bar = 50 μm. (b) The proportion of the seminiferous tubules with apoptotic germ cells was determined. Over 180 tubules per group were analyzed in three mice and were statistically analyzed with two-way ANOVA. The values are means and *SEM*. ANOVA, analysis of varaince; DAPI, 4′,6-diamidino-2-phenylindole; *SEM*, standard error of mean; TUNEL, terminal deoxynucleotidyl transferase dUTP nick end labeling. $^{*}p < .05$; $^{**}p < .01$; $^{****}p < .0001$

apoptosis most abundantly in the mid-testicular stages (VII–VIII) and less extensively in late testicular-stage spermatocytes (IX–XII; Figure 3b). Germ cell apoptosis in the early testicular stages (I–VI) was minimal (Figure 3b). These results suggest that male germ cells at specific tubular stages (VII–VIII) are more susceptible to heat stress than those at other stages.

2.4 | BTB leakage in tubular stages VII–VIII

To examine why spermatocytes in tubular stages VII–VIII are most vulnerable to apoptosis upon heat stress, we focused on the fact that BTB is reorganized in the mid-stage of the seminiferous tubules (Siu, Mruk, Porto, & Cheng, 2009). Since preleptotene spermatocytes in the basal compartment need to migrate into the adluminal compartment during development, the BTB must be transiently reorganized during testicular stages VII–VIII (Wen et al., 2018). To determine BTB integrity, we performed biotin-tracer assays, in which a fluorescently labeled small molecule, such as biotin penetrates through the BTB from the basal compartment to the adluminal space (Meng, Holdcraft, Shima, Griswold, & Braun, 2005). Cadmium chloride ($CdCl_2$) was used as a positive control for BTB disturbance (Su, Mruk, & Cheng, 2011). The results showed that prolonged severe heat stress (42°C for 6 hr) increased biotin penetration in tubules at all stages, but most significantly in tubules at mid-testicular stages VII–VIII (Figure 4a,b). We further performed immunostaining analyses to determine BTB integrity in seminiferous tubules at stages VII–VIII by examining Sertoli cell morphology upon prolonged heat

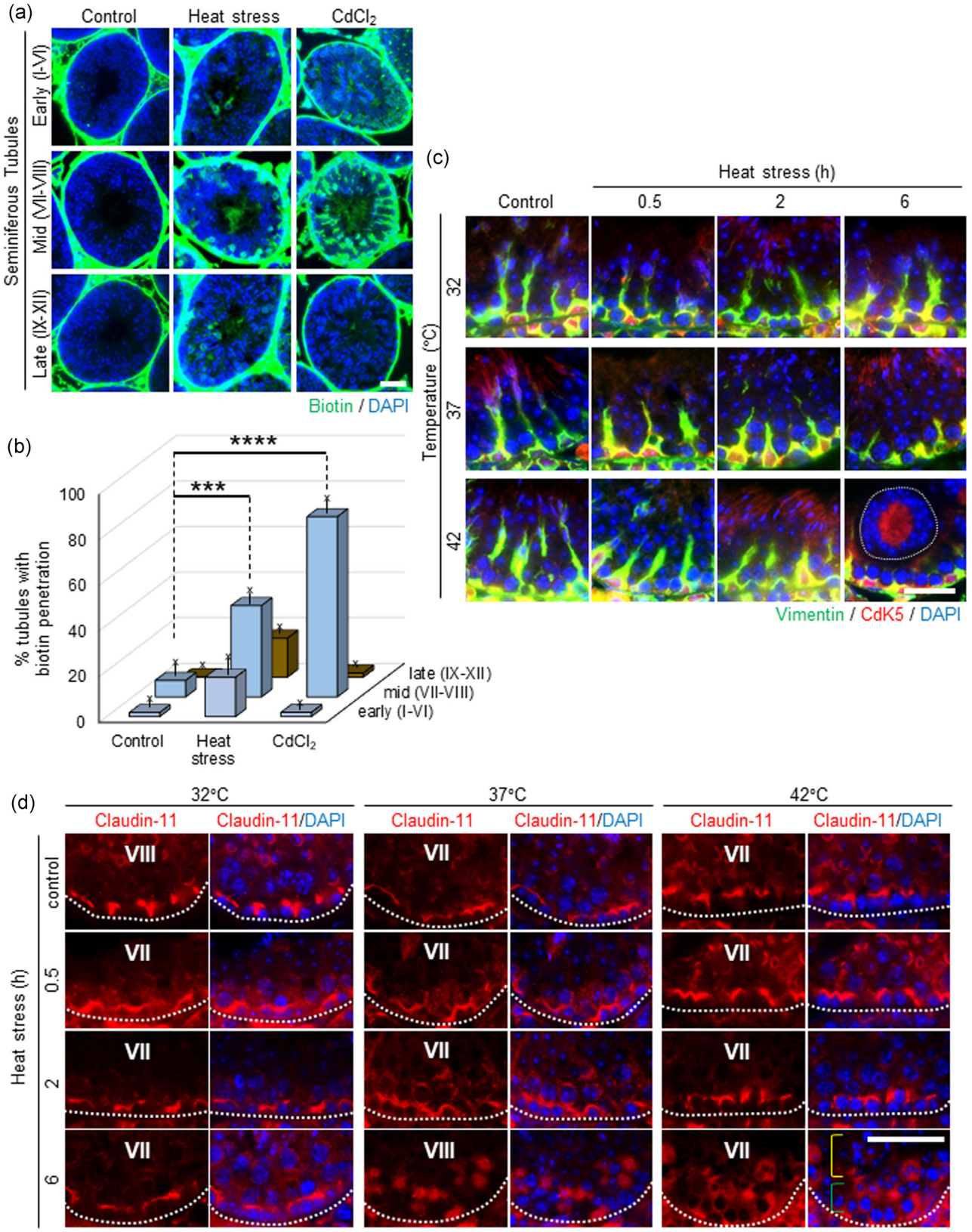
(a)
Control
Heat stress
CdCl2
Seminiferous Tubules
Early (I-VI)
Mid (VII-VIII)
Late (IX-XII)
Biotin / DAPI
(b)
****
***
% tubules with biotin penetration
100
80
60
40
20
0
Control
Heat stress
CdCl2
late (IX-XII)
mid (VII-VIII)
early (I-VI)
(c)
Heat stress (h)
Control
0.5
2
6
Temperature (°C)
32
37
42
Vimentin / CdK5 / DAPI
(d)
32°C
37°C
42°C
Claudin-11
Claudin-11/DAPI
Heat stress (h)
control
0.5
2
6
VIII
VII

stress (42°C for 6 hr). Sertoli cells, which were immunostained with vimentin and cyclin-dependent kinase 5 (Cdk5), were fully stretched out and tightly linked at the periphery of mid-stage seminiferous tubules, suggesting that the tight junctions were properly organized among these cells (Figure 4c). However, the vimentin and Cdk5 signals between sertoli cells were disrupted in the heat-stressed testes. The cytoskeletal structures of Sertoli cells were further disturbed under severe heat stress at 42°C, forming abnormal multinucleated giant cells (Figure 4c). Claudin-11, a tight junction protein, was also abnormally diffused into the adluminal compartment from the basal compartment of mid-stage (VII–VIII) seminiferous tubules after prolonged heat exposure (37–42°C for 6 hr; Figure 4d). These results indicate that prolonged heat stress (42°C for 6 hr) disturbs BTB integrity, especially in seminiferous tubules at stages VII–VIII.

2.5 | Effects of BTB leakage on germ cell apoptosis upon heat stress

Since we observed BTB leakage upon heat stress, we next examined whether this leakage was attributed to germ cell apoptosis after prolonged heat stress (42°C for 6 hr). First, we determined the effects of $CdCl_2$ on germ cell apoptosis. As expected, cadmium-induced BTB leakage did not cause significant damage to the overall testis morphology (Figure 5a,b). We also observed that prolonged heat stress (42°C for 6 hr) induced BTB leakage, but not as much as cadmium did (Figure 5b,c). However, the combined treatment of cadmium and heat stress was extremely deleterious, and the germ cell layers were markedly disorganized overall; detachment of spermatogonia and spermatocytes from the basal membrane and deep clefts were also observed (Figure 5a). Germ cell apoptosis was observed with cadmium treatment; however, spermatocyte apoptosis particularly increased with cadmium treatment upon prolonged heat stress (42°C for 6 hr; Figure 5d,e). These results indicate that the testis tissue disturbed by BTB leakage contributes to germ cell apoptosis synergistically with prolonged heat stress (42°C for 6 hr).

3 | DISCUSSION

In this study, we analyzed the effects of whole-body heat exposure on the mouse testis. We observed that heat-induced stress responses directly within germ cells, such as eIF2α phosphorylation and SG formation. Further, tissue organization in the testis was disturbed by our heat treatment schemes, and the BTB was critically disturbed after prolonged heat exposure (42°C for 6 hr). Collectively, our results suggest that heat-induced tissue disorganization may synergistically escalate the incidence of male germ cell death (Figure 6).

Interestingly, male germ cells respond differently to heat stress in a developmental stage-specific manner. Among male germ cells, spermatocytes are the most sensitive to heat stress (Kim et al., 2012; Yoon et al., 2017), and those near meiosis are particularly susceptible (Dunkel, Hirvonen, & Erkkila, 1997; Kim et al., 2012; Lue et al., 1999). We also observed that a significant proportion of the spermatocytes at tubular stages IX–XII underwent apoptosis following whole-body heat exposure, as shown in Figure 3. In contrast, the spermatocytes at early tubular stages (I–VI) were relatively resistant to heat stress. This may be due to the presence of a protective mechanism against heat stress in early tubular-stage spermatocytes (Kim et al., 2012; Yoon et al., 2017); in fact, Dazl, an important factor for SG formation, is specifically expressed in such spermatocytes (Kim et al., 2012). Finally, apoptosis was most frequently detected in spermatocytes in the mid-stage (VII–VIII) seminiferous tubules (Figure 3).

Notably, SGs dissolved in 2 hr under severe heat treatment. It is known that eIF2α phosphorylation is linked to SG formation during heat stress (Yoon et al., 2017). However, there may not be a linear correlation between phospho-eIF2α levels in testicular lysates and SG formation rates. The elevation of eIF2α phosphorylation following heat stress at 37°C may initiate other well-known stress responses, such as endoplasmic reticulum stress responses, rather than recruiting SGs for heat protection (Bettaieb & Averill-Bates, 2015). Even if they are transient, SGs should still play a role in protecting germ cells against apoptosis (Figure 2).

We doubt that spermatocytes in mid-stage tubules are more sensitive to heat stress than those in other stages. In fact, it has been proposed that testosterone protects germ cells in tubular stages VII–VIII against heat-induced apoptosis (Lue et al., 1999). The proportions of apoptotic spermatocytes at tubular stages VII–VIII are comparable to those at tubular stages IX–XII under diverse stress treatments, including GnRH antagonist and heat (Spriggs, Bushell, & Willis, 2010). Rather, we suspect that prolonged heat stress (42°C for 6 hr) might affect testicular tissue organization at tubular stages VII–VIII; in fact, during these stages, the BTB is reorganized to allow preleptotene spermatocytes to pass through the barrier for further

FIGURE 4 Leakage of the blood-testis barrier (BTB) upon prolonged heat stress. (a) Mice were treated with $CdCl_2$ (3 mg/kg for 24 hr) or prolonged heat (42°C for 6 hr), and their testes were subjected to biotin-tracer assay (green). Seminiferous tubules were grouped into early (I–VI), mid (VII–VIII), and late (IX–XII) stages based on DAPI staining (blue). Scale bar = 50 μm. (b) The biotin-penetrated seminiferous tubules were counted. Over 180 tubules were analyzed in three mice and were statistically analyzed with two-way ANOVA. The values are means and *SEM*. ***$p < .001$; ****$p < .0001$. (c) Testis sections from the heat-stressed mice were immunostained with antibodies specific to vimentin (green) and Cdk5 (red). A multinucleated giant cell is surrounded by a white dashed line. Scale bar = 50 μm. (d) BTB integrity was specifically examined in stages VII–VIII after prolonged heat shock. Claudin-11 (red) was stained to mark a tight junction component of the BTB. DNA was stained with DAPI (blue). Green and yellow square brackets indicate the basal and adluminal compartments, respectively. Dashed lines indicate the basal membrane of the seminiferous tubules. Scale bars = 50 μm. ANOVA, analysis of variance; Cdk5, cyclin-dependent kinase 5; DAPI, 4′,6-diamidino-2-phenylindole; *SEM*, standard error of mean

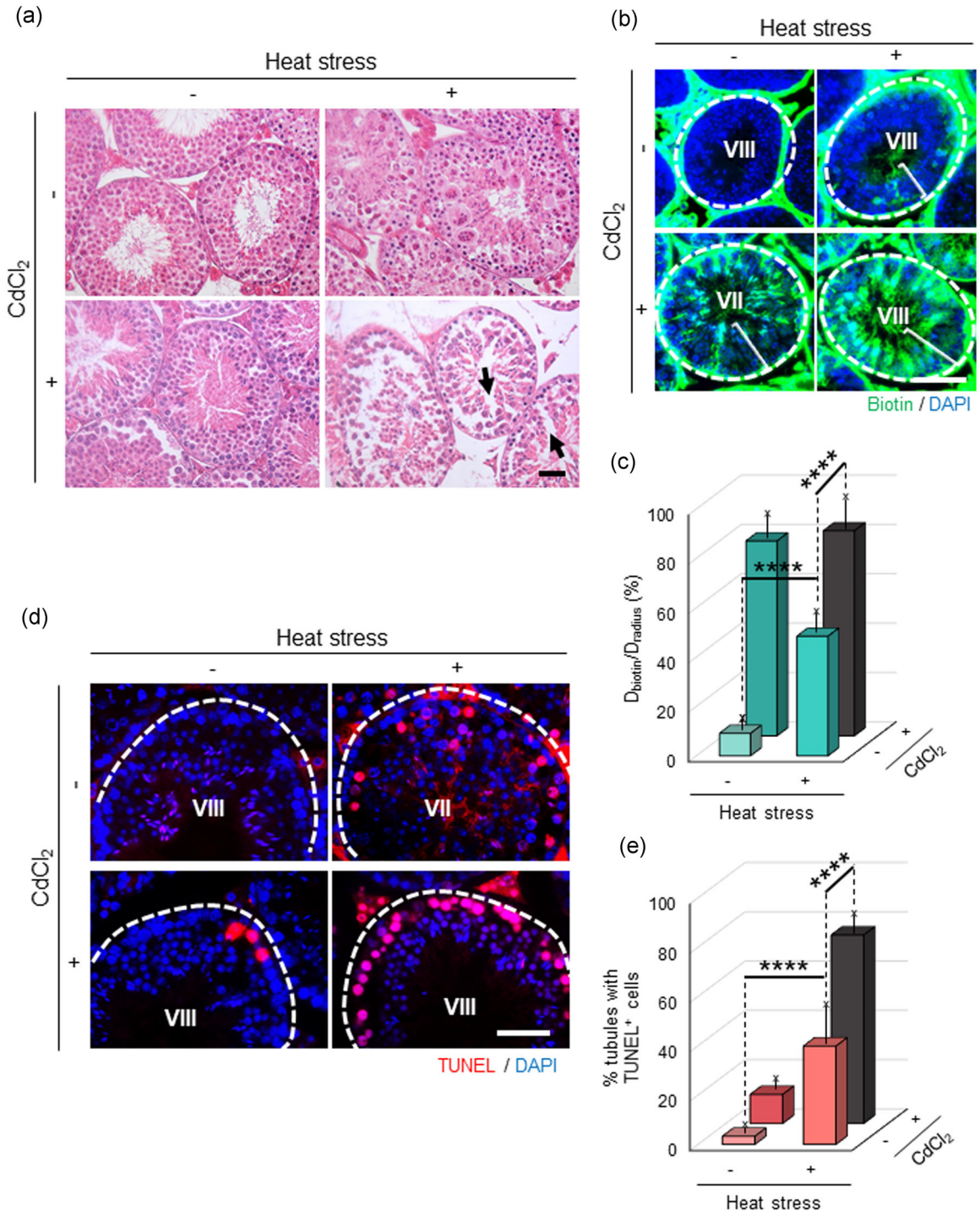

FIGURE 5 The synergistic effect of cadmium and prolonged heat stress on germ cell apoptosis. (a) Mice were simultaneously treated with $CdCl_2$ (3 mg/kg for 24 hr) and prolonged heat (42°C for 6 hr), and their testes were subjected to H&E staining. Black arrows indicate the deep clefts of the seminiferous tubules. Scale bar = 50 μm. (b) Biotin-tracer assays were performed in VII–VIII seminiferous tubules (green). DNA was stained with DAPI (blue). Broken circles and square brackets indicate seminiferous tubule outlines and the distance penetrated by biotin, respectively. (c) The relative distances traveled by biotin in the seminiferous tubules (D_{biotin}/D_{radius}) were determined. Over 180 tubules were analyzed in three mice and were statistically analyzed using one-way ANOVA. (d) TUNEL assays were performed in VII–VIII seminiferous tubules (red). DNA was stained with DAPI (blue). (e) Seminiferous tubules with apoptotic germ cells were counted. Over 40 tubules per group were analyzed in three mice and statistically analyzed using one-way ANOVA. The values are the means and *SEM*. ANOVA, analysis of variance; DAPI, 4′,6-diamidino-2-phenylindole; H&E, hematoxylin & eosin; *SEM*, standard error of mean; TUNEL, terminal deoxynucleotidyl transferase dUTP nick end labeling. ****$p < .0001$

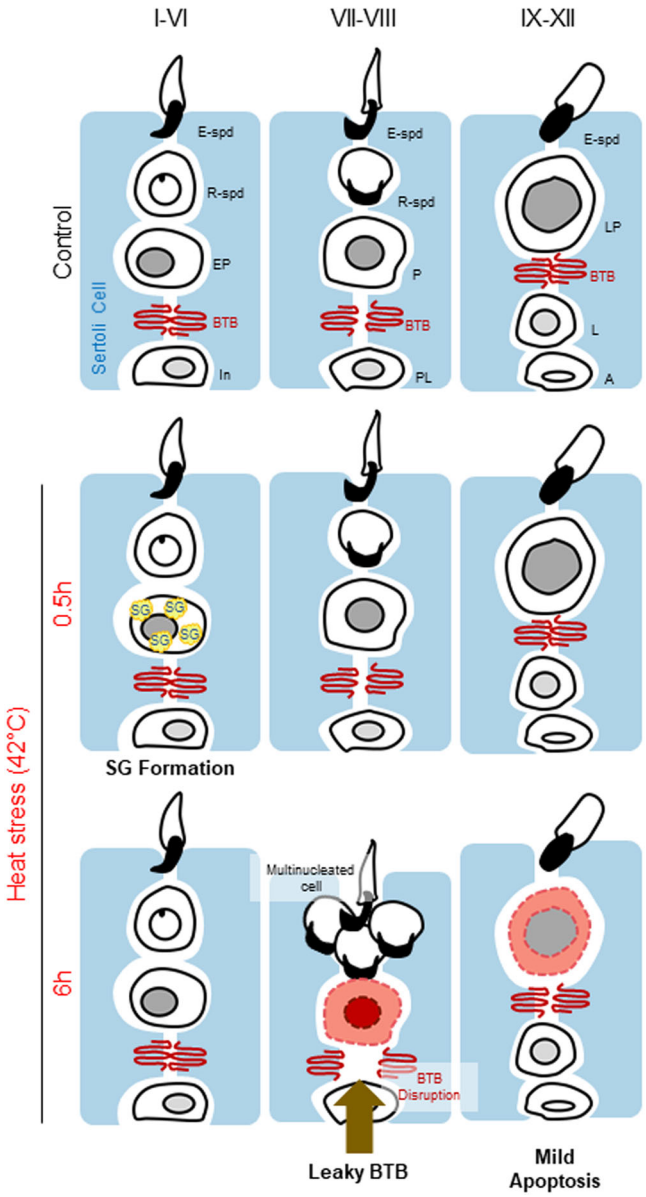

FIGURE 6 Model. Heat stress induces multiple stress responses in mouse male germ cells. Of germ cells, spermatocytes are the most vulnerable to heat stress. However, the adverse effects of heat stress on spermatocytes are not identical throughout their developmental stages. Spermatocytes in the early tubular stages (I–VI) form SGs for protection against heat stress. In the mid-tubular stages (VII–VIII), BTB leakage synergistically enhances the adverse effects of heat stress on spermatocyte apoptosis. In the late tubular stages (IX–XII), SGs are not formed, nor does severe BTB leakage occur, resulting in mild apoptosis of spermatocytes near meiosis. The arrow indicates biotin penetration. A, spermatogonia; BTB, blood-testis barrier; EP, early pachytene spermatocyte; E-Spd, elongated spermatid; In, intermediate spermatogonia; L, leptotene spermatocyte; LP, late pachytene spermatocyte; P, pachytene spermatocyte; PL, preleptotene spermatocyte; R-Spd, round spermatid; SG, stress granule

development into pachytene spermatocytes (Wan, Mruk, Wong, & Cheng, 2013). Collectively, prolonged heat exposure (42°C for 6 hr) might affect the BTB reorganization process and may significantly disrupt the overall testis morphology, thus generating abnormal cell types, such as multinucleated giant germ cells. These multinucleated giant germ cells showed spermatogenic stage-specific formation, which differed from the non-stage-specific formation due to spermatogenic arrest in cryptorchid mouse testes with chronic heat exposure (Bianchi, Boekelheide, Sigman, Hall, & Hwang, 2017).

Sertoli cell integrity is essential for germ cell development, as disruption of these cells results in defects in germ cell morphology and survival (Elkin, Piner, & Sharpe, 2010; ErLin et al., 2015; Murphy & Richburg, 2014; Siu et al., 2009; Wen et al., 2018). Repetitive heat exposure did not affect sertoli cell survival (Valles, Aveldano, & Furland, 2014). While such changes are temporary and potentially reversible, heat stress induces structural and metabolic alterations in the secretion and cytoskeletal organization of sertoli cells (Valles et al., 2014). Disruption of BTB integrity is one possible outcome in sertoli cells after heat stress (Cai et al., 2011).

Even if disruption of the BTB causes damage in testis tissues, this disruption may not be the whole reason for germ cell apoptosis upon heat stress. Accordingly, we observed that BTB disruption alone did not induce spermatocyte apoptosis as effectively as prolonged heat stress (42°C for 6 hr). However, we observed deleterious outcomes in germ cell apoptosis when mice were exposed to heat in the presence of a BTB disruptor (Figure 5). Based on these observations, we propose that BTB disruption enforces the adverse effects of prolonged heat stress (42°C for 6 hr) on mid-tubular-stage spermatocytes. Once the testicular tissue microenvironment is damaged, spermatocytes become more vulnerable to heat stress and easily undergo apoptosis (Figure 6).

We concluded that the synergistic effects of BTB disruption on germ cell apoptosis were detected only when testes were exposed to heat (42°C) for a prolonged time period (6 hr). In fact, we and others previously observed stress responses in male germ cells only after short-term heat treatment. Detailed mechanisms of the spatio-temporal dynamics of germ cells against thermal stress remain to be elucidated. Furthermore, it is also important to determine how the damaged microenvironment of the testis is recovered.

4 | MATERIALS AND METHODS

4.1 | Animals

All animal treatments were performed in accordance with the relevant guidelines and regulations approved by the Institutional Animal Care and Use Committee at Seoul National University, Korea (Permit Number SNU-180219-3). All animals used in this experiment were housed with a 12-hr light and dark cycle at proper temperature, and sufficient food and sterilized water were provided. C57BL/6 adult male mice (12 weeks old) were used for all heat treatment experiments.

4.2 | Heat treatment

For whole-body heat treatment, C57BL/6 adult male mice were placed in a large warming/induction chamber (Animal Identification

and Marking Systems, Inc., Hornell, NY) in the presence of water and food. Each heat-stressed mouse group ($n = 3$) was maintained at a different temperature (32, 37, or 42°C) for a short-term period (0.5 and 2 hr) or an extended period (6 hr). Sham control mice were also caged in the same warming chamber at room temperature (25 ± 2°C) for 6 hr. After the treatments, the mice from both heat-stressed and control groups were killed in a CO_2 chamber. To delineate the potential effect of stress due to the new environment, mice were acclimatized to the warming chamber for 12 hr at room temperature before the actual examination.

4.3 | Spermatogenic cycle determination

The morphologies and sizes of germ cell nuclei stained with DAPI and hematoxylin were used to isolate specific phases of spermatogenesis. According to the shapes of spermatid nuclei, 12 seminiferous stages can be divided into early (I–IV; Step 13–15 spermatids), mid (VII–VIII; Step 16 spermatid), and late (IX–XII; Step 9–12 spermatids) phases (Figure S1; Hess & Renato de Franca, 2008). After adapting the method of Bazille et al. (2005), we observed that stages I–VI, VII–VII, and IX–XII contained round spermatids, preleptotene spermatocytes, and meiotic spermatocytes, respectively (Bazille et al., 2005).

4.4 | $CdCl_2$ treatment

$CdCl_2$ was purchased from Sigma-Aldrich (#439800; St. Louis, MO), diluted in 0.9% NaCl solution, and administered to mice ($n = 6$) with a single dose of 3 mg/kg via intraperitoneal injection. Vehicle mice ($n = 3$) were treated with 0.9% NaCl solution only. After 24 hr, the mice ($n = 3$) were placed in warming chambers for 6 hr at 25 or 42°C and then killed.

4.5 | Immunoblot analysis

Mouse testicular samples were homogenized with radioimmunoprecipitation assay buffer (150 mM NaCl, 50 mM Tris pH 8.0, 1 mM ethylenediaminetetraacetic acid, 1 mM ethylene glycol-bis(β-aminoethyl ether)-*N*,*N*,*N*′,*N*′-tetraacetic acid, 1.0% NP-40, 0.5% sodium deoxycholate, 0.1% sodium dodecyl sulfate (SDS), 10 mM NaF, 1 mM NaV, and a protease inhibitor cocktail) and were centrifuged to remove debris. The supernatant lysates were mixed with 2X SDS-polyacrylamide gel electrophoresis sample buffer, loaded on 9–10% SDS-polyacrylamide gels, and resolved by electrophoresis. The separated proteins were transferred to nitrocellulose membranes. The blots were blocked in 5% bovine serum albumin (BSA) or 5% skimmed milk in 0.1% Tris-buffered saline with Tween-20 (TBST; 20 mM Tris pH 7.3, 150 mM NaCl, and 0.1% Tween-20) and then incubated with the indicated antibodies with proper titers overnight at 4°C. The next day, the blot was washed three times with TBST and then incubated with peroxidase-conjugated secondary antibodies for 30 min at room temperature. The blot was again washed with TBST and then exposed to ECL reagents to visualize the protein bands. The titers of the primary antibodies were as follows: p-eIF2α (1:150; #ab32157; Abcam, Cambridge, UK), eIF2α (1:150, #sc-11386; Santa Cruz Biotechnology, Santa Cruz, CA), and PARP (1:1,000, #9542; Cell Signaling Technology, Danvers, MA).

4.6 | Immunofluorescence staining

Control and whole-body heat-treated mice were killed, and the testes were fixed in Bouin's solution (Sigma-Aldrich) overnight at 4°C. Fixed testes were embedded in paraffin and sectioned at 5-μm thickness. The testis sections were boiled for antigen retrieval (30 min). Slides were blocked with 0.1% phosphate-buffered saline with 0.1% Triton X-100 (PBST) containing 3% BSA for 30 min and then incubated with primary antibodies overnight at 4°C. The antibodies used for immunohistochemistry were as follows: vimentin (1:100, #ab9247; Abcam), Cdk5 (1:100, #sc-6247; Santa Cruz Biotechnology), Claudin-11 (1:20, #36–4500; Invitrogen, Carlsbad, CA), TIA-1 (1:25, #sc-1751; Santa Cruz Biotechnology), and Dazl (1:10; manufactured in Rhee's lab; Kim et al., 2012). After the testis sections were washed with PBST, they were incubated with either fluorophore-conjugated (Invitrogen) or biotinylated secondary antibodies (Vector Laboratories, Burlingame, CA) for 30 min at room temperature. Then, the samples were incubated with DAPI for 30 s before being mounted (ProLong Gold, Thermo Fisher Scientific, Waltham, MA).

4.7 | H&E staining

Control and whole-body heat-treated mice were killed, and the testis, lung, jejunum, and brain tissues were excised for staining. All tissues were fixed in Bouin's solution (Sigma-Aldrich) overnight at 4°C before paraffin processing. All sections were 5-μm thick, and H&E staining was conducted using an automatic staining machine (Leica ST5010 Autostainer XL, Leica, Wetzlar, Germany).

4.8 | TUNEL assay

TUNEL assay was performed to detect germ cell apoptosis. The FragEL DNA Fragmentation Detection Kit (cat. no. Q1A39; Calbiochem, San Diego, CA) was used, and the manufacturer's instructions were strictly followed. In brief, the rehydrated testicular sections were permeabilized with proteinase K and treated with 1X terminal deoxynucleotidyl transferase equilibrium buffer to tag the exposed 3′-OH ends of DNA fragments.

4.9 | Biotin-tracer assay

Control mice and mice exposed to prolonged heat stress (42°C for 6 hr) were anesthetized, and the testes were exposed. Fresh 50 μl

EZ-Link Sulfo-NHS-LC-Biotin (10 mg/ml in PBS containing 1 mM $CaCl_2$; #21335; Thermo Fisher Scientific) was injected into the testis interstitium. After 30 min of incubation, the mice were killed by CO_2 asphyxiation. Extracted testes were fixed in Bouin's solution overnight and embedded in a paraffin block. Testicular tissue was sectioned at 5-μm thickness. After deparaffinization, the slides were blocked with 5% BSA diluted in PBST. Finally, the sections were incubated with Alexa Fluor 568-conjugated streptavidin (1:200, #S32354; Invitrogen) for 40 min at room temperature to visualize the biotin signals through fluorescence microscopy after mounting. BTB permeability was assessed by tracing the biotin signal; the distance that the biotin signal traveled from the testicular basal membrane to the adluminal direction (D_{biotin}) was divided by the average radius of each corresponding seminiferous tubule (D_{radius}).

4.10 | Imaging

Immunofluorescence images were obtained using a fluorescence microscope (Olympus IX51 equipped with QImaging QICAM Fast 1394 Olympus, Tokyo, Japan), and H&E staining results were acquired using a light microscope (Olympus BX51). The acquired images were processed with ImagePro 5.0 (Media Cybernetics, Rockville, MD), ProgRes CapturePro V2.8.8 (JENOPTIK, Jena, Germany), ImageJ 1.52 (National Institutes of Health, Bethesda, MD), and Photoshop CS6 (Adobe, San Jose, CA). The best representative image was selected from at least three independent experiments.

4.11 | Statistical analysis

Quantitative data are presented as the mean ± standard error of mean. Statistical significance was analyzed using one-way analysis of variance (ANOVA) or two-way ANOVA. A $p < .05$ shows statistical significance.

ACKNOWLEDGMENT

This research was supported by the Basic Science Research Program through the National Research Foundation of Korea funded by the Ministry (NRF-2019R1A2C2002726).

CONFLICT OF INTERESTS

The authors declare that there are no conflict of interests.

ORCID

Kunsoo Rhee http://orcid.org/0000-0002-5051-876X

REFERENCES

Alam, M. S., & Kurohmaru, M. (2014). Disruption of Sertoli cell vimentin filaments in prepubertal rats: An acute effect of butylparaben in vivo and in vitro. *Acta Histochemica*, *116*(5), 682–687. https://doi.org/10.1016/j.acthis.2013.12.006

Anderson, P., & Kedersha, N. (2008). Stress granules: The Tao of RNA triage. *Trends in Biochemical Sciences*, *33*(3), 141–150. https://doi.org/10.1016/j.tibs.2007.12.003

Baler, R., Dahl, G., & Voellmy, R. (1993). Activation of human heat shock genes is accompanied by oligomerization, modification, and rapid translocation of heat shock transcription factor HSF1. *Molecular and Cellular Biology*, *13*(4), 2486–2496. https://doi.org/10.1128/mcb.13.4.2486

Bazille, C., Megarbane, B., Bensimhon, D., Lavergne-Slove, A., Baglin, A. C., Loirat, P., … Gray, F. (2005). Brain damage after heat stroke. *Journal of Neuropathology and Experimental Neurology*, *64*(11), 970–975. https://doi.org/10.1097/01.jnen.0000186924.88333.0d

Bettaieb, A., & Averill-Bates, D. A. (2015). Thermotolerance induced at a mild temperature of 40 degrees C alleviates heat shock-induced ER stress and apoptosis in HeLa cells. *Biochimica et Biophysica Acta/General Subjects*, *1853*(1), 52–62. https://doi.org/10.1016/j.bbamcr.2014.09.016

Bianchi, E., Boekelheide, K., Sigman, M., Hall, S. J., & Hwang, K. (2017). Ghrelin modulates testicular damage in a cryptorchid mouse model. *PLoS One*, *12*(5):e0177995. https://doi.org/10.1371/journal.pone.0177995

Cai, H., Ren, Y., Li, X. X., Yang, J. L., Zhang, C. P., Chen, M., … Liu, Y. X. (2011). Scrotal heat stress causes a transient alteration in tight junctions and induction of TGF-beta expression. *International Journal of Andrology*, *34*(4), 352–362. https://doi.org/10.1111/j.1365-2605.2010.01089.x

Cataldo, L., Mastrangelo, M. A., & Kleene, K. C. (1997). Differential effects of heat shock on translation of normal mRNAs in primary spermatocytes, elongated spermatids, and Sertoli cells in seminiferous tubule culture. *Experimental Cell Research*, *231*(1), 206–213. https://doi.org/10.1006/excr.1996.3447

Dayalan Naidu, S., & Dinkova-Kostova, A. T. (2017). Regulation of the mammalian heat shock factor 1. *FEBS Journal*, *284*(11), 1606–1627. https://doi.org/10.1111/febs.13999

DeFoor, W. R., Kuan, C. Y., Pinkerton, M., Sheldon, C. A., & Lewis, A. G. (2004). Modulation of germ cell apoptosis with a nitric oxide synthase inhibitor in a murine model of congenital cryptorchidism. *Journal of Urology*, *172*(4 Pt 2), 1731–1735.

Dunkel, L., Hirvonen, V., & Erkkila, K. (1997). Clinical aspects of male germ cell apoptosis during testis development and spermatogenesis. *Cell Death & Differentiation*, *4*(3), 171–179. https://doi.org/10.1038/sj.cdd.4400234

Durairajanayagam, D., Agarwal, A., & Ong, C. (2015). Causes, effects, and molecular mechanisms of testicular heat stress. *Reproductive BioMedicine Online*, *30*(1), 14–27. https://doi.org/10.1016/j.rbmo.2014.09.018

Elkin, N. D., Piner, J. A., & Sharpe, R. M. (2010). Toxicant-induced leakage of germ cell-specific proteins from seminiferous tubules in the rat: Relationship to blood-testis barrier integrity and prospects for biomonitoring. *Toxicological Sciences*, *117*(2), 439–448. https://doi.org/10.1093/toxsci/kfq210

ErLin, S., WenJie, W., LiNing, W., BingXin, L., MingDe, L., Yan, S., & RuiFa, H. (2015). Musashi-1 maintains blood-testis barrier structure during spermatogenesis and regulates stress granule formation upon heat stress. *Molecular Biology of the Cell*, *26*(10), 1947–1956. https://doi.org/10.1091/mbc.E14-11-1497

Hansen, P. J. (2009). Effects of heat stress on mammalian reproduction. *Philosophical Transactions of the Royal Society of London. Series B, Biological Sciences*, *364*(1534), 3341–3350. https://doi.org/10.1098/rstb.2009.0131

Hess, R. A., & Renato de Franca, L. (2008). Spermatogenesis and cycle of the seminiferous epithelium. *Advances in Experimental Medicine and Biology*, *636*, 1–15. https://doi.org/10.1007/978-0-387-09597-4_1

Hifumi, T., Kondo, Y., Shimizu, K., & Miyake, Y. (2018). Heat stroke. *Journal of Intensive Care*, *6*, 30. https://doi.org/10.1186/s40560-018-0298-4

Hogarth, C. A., & Griswold, M. D. (2010). The key role of vitamin A in spermatogenesis. *Journal of Clinical Investigation*, *120*(4), 956–962. https://doi.org/10.1172/JCI41303

Houston, B. J., Nixon, B., Martin, J. H., De Iuliis, G. N., Trigg, N. A., Bromfield, E. G., … Aitken, R. J. (2018). Heat exposure induces oxidative stress and DNA damage in the male germ line. *Biology of Reproduction*, *98*(4), 593–606. https://doi.org/10.1093/biolre/ioy009

Ishikawa, T., Kondo, Y., Goda, K., & Fujisawa, M. (2005). Overexpression of endothelial nitric oxide synthase in transgenic mice accelerates testicular germ cell apoptosis induced by experimental cryptorchidism. *Journal of Andrology*, *26*(2), 281–288.

Kim, B., Cooke, H. J., & Rhee, K. (2012). DAZL is essential for stress granule formation implicated in germ cell survival upon heat stress. *Development*, *139*(3), 568–578. https://doi.org/10.1242/dev.075846

Kim, B., Park, K., & Rhee, K. (2013). Heat stress response of male germ cells. *Cellular and Molecular Life Sciences*, *70*(15), 2623–2636. https://doi.org/10.1007/s00018-012-1165-4

Li, L., Tan, H., Gu, Z., Liu, Z., Geng, Y., Liu, Y., … Su, L. (2014). Heat stress induces apoptosis through a Ca(2)(+)-mediated mitochondrial apoptotic pathway in human umbilical vein endothelial cells. *PLoS One*, *9*(12):e111083. https://doi.org/10.1371/journal.pone.0111083

Liu, Z. F., Li, B. L., Tong, H. S., Tang, Y. Q., Xu, Q. L., Guo, J. Q., & Su, L. (2011). Pathological changes in the lung and brain of mice during heat stress and cooling treatment. *World Journal of Emergency Medicine*, *2*(1), 50–53.

Lue, Y. H., Hikim, A. P., Swerdloff, R. S., Im, P., Taing, K. S., Bui, T., … Wang, C. (1999). Single exposure to heat induces stage-specific germ cell apoptosis in rats: Role of intratesticular testosterone on stage specificity. *Endocrinology*, *140*(4), 1709–1717. https://doi.org/10.1210/endo.140.4.6629

Luo, L., Li, Y., Yang, Y., He, Y., Wang, Y., Xu, Z., & Zhang, Y. (2013). Multinucleated cells are involved in normal development and apoptosis in mouse testes. *Molecular Medicine Reports*, *8*(3), 865–870. https://doi.org/10.3892/mmr.2013.1568

Meistrich, M. L., & Hess, R. A. (2013). Assessment of spermatogenesis through staging of seminiferous tubules. *Methods in Molecular Biology*, *927*, 299–307. https://doi.org/10.1007/978-1-62703-038-0_27

Meng, J., Holdcraft, R. W., Shima, J. E., Griswold, M. D., & Braun, R. E. (2005). Androgens regulate the permeability of the blood-testis barrier. *Proceedings of the National Academy of Sciences of the United States of America*, *102*(46), 16696–16700. https://doi.org/10.1073/pnas.0506084102

Morrow, C. M., Mruk, D., Cheng, C. Y., & Hess, R. A. (2010). Claudin and occludin expression and function in the seminiferous epithelium. *Philosophical Transactions of the Royal Society of London. Series B, Biological Sciences*, *365*(1546), 1679–1696. https://doi.org/10.1098/rstb.2010.0025

Mruk, D. D., & Cheng, C. Y. (2015). The mammalian blood-testis barrier: Its biology and regulation. *Endocrine Reviews*, *36*(5), 564–591. https://doi.org/10.1210/er.2014-1101

Murphy, C. J., & Richburg, J. H. (2014). Implications of sertoli cell induced germ cell apoptosis to testicular pathology. *Spermatogenesis*, *4*(2): e979110. https://doi.org/10.4161/21565562.2014.979110

Nakamura, M., & Hall, P. F. (1980). The mechanism by which body temperature inhibits protein biosynthesis in spermatids of rat testes. *Journal of Biological Chemistry*, *255*(7), 2907–2913.

Pabst, D. A., Rommel, S. A., McLellan, W. A., Williams, T. M., & Rowles, T. K. (1995). Thermoregulation of the intra-abdominal testes of the bottlenose dolphin (*Tursiops truncatus*) during exercise. *Journal of Experimental Biology*, *198*(Pt 1), 221–226.

Reitman, M. L. (2018). Of mice and men—environmental temperature, body temperature, and treatment of obesity. *FEBS Letters*, *592*(12), 2098–2107. https://doi.org/10.1002/1873-3468.13070

Roberts, G. T., Ghebeh, H., Chishti, M. A., Al-Mohanna, F., El-Sayed, R., Al-Mohanna, F., & Bouchama, A. (2008). Microvascular injury, thrombosis, inflammation, and apoptosis in the pathogenesis of heatstroke: A study in baboon model. *Arteriosclerosis, Thrombosis, and Vascular Biology*, *28*(6), 1130–1136. https://doi.org/10.1161/ATVBAHA.107.158709

Session, D. R., Fautsch, M. P., Avula, R., Jones, W. R., Nehra, A., & Wieben, E. D. (2001). Cyclin-dependent kinase 5 is expressed in both sertoli cells and metaphase spermatocytes. *Fertility and Sterility*, *75*(4), 669–673.

Siu, E. R., Mruk, D. D., Porto, C. S., & Cheng, C. Y. (2009). Cadmium-induced testicular injury. *Toxicology and Applied Pharmacology*, *238*(3), 240–249. https://doi.org/10.1016/j.taap.2009.01.028

Spriggs, K. A., Bushell, M., & Willis, A. E. (2010). Translational regulation of gene expression during conditions of cell stress. *Molecular Cell*, *40*(2), 228–237. https://doi.org/10.1016/j.molcel.2010.09.028

Su, L., Mruk, D. D., & Cheng, C. Y. (2011). Drug transporters, the blood-testis barrier, and spermatogenesis. *Journal of Endocrinology*, *208*(3), 207–223. https://doi.org/10.1677/JOE-10-0363

Valles, A. S., Aveldano, M. I., & Furland, N. E. (2014). Altered lipid homeostasis in Sertoli cells stressed by mild hyperthermia. *PLoS One*, *9*(4):e91127. https://doi.org/10.1371/journal.pone.0091127

Ventela, S., Ohta, H., Parvinen, M., & Nishimune, Y. (2002). Development of the stages of the cycle in mouse seminiferous epithelium after transplantation of green fluorescent protein-labeled spermatogonial stem cells. *Biology of Reproduction*, *66*(5), 1422–1429.

Vydra, N., Malusecka, E., Jarzab, M., Lisowska, K., Glowala-Kosinska, M., Benedyk, K., … Widlak, W. (2006). Spermatocyte-specific expression of constitutively active heat shock factor 1 induces HSP70i-resistant apoptosis in male germ cells. *Cell Death & Differentiation*, *13*(2), 212–222. https://doi.org/10.1038/sj.cdd.4401758

Wan, H. T., Mruk, D. D., Wong, C. K., & Cheng, C. Y. (2013). The apical ES-BTB-BM functional axis is an emerging target for toxicant-induced infertility. *Trends in Molecular Medicine*, *19*(7), 396–405. https://doi.org/10.1016/j.molmed.2013.03.006

Wang, Y. H., Liu, T. T., Kung, W. M., Chen, C. C., Wen, Y. T., Lin, I. C., … Wei, L. (2015). Expression of aquaporins in intestine after heat stroke. *International journal of clinical and experimental pathology*, *8*(8), 8742–8753.

Wen, Q., Li, N., Xiao, X., Lui, W. Y., Chu, D. S., Wong, C. K. C., … Cheng, C. Y. (2018). Actin nucleator Spire 1 is a regulator of ectoplasmic specialization in the testis. *Cell Death & Disease*, *9*(2), 208. https://doi.org/10.1038/s41419-017-0201-6

Yoon, J., Park, K., Hwang, D. S., & Rhee, K. (2017). Importance of eIF2alpha phosphorylation as a protective mechanism against heat stress in mouse male germ cells. *Molecular Reproduction and Development*, *84*(3), 265–274. https://doi.org/10.1002/mrd.22778

Zhao, J., Zhang, Y., Hao, L., Wang, J., Zhang, J., Liu, S., & Ren, B. (2010). Effects of a mild heat treatment on mouse testicular gene expression and sperm quality. *Animal Cells Syst*, *14*(4), 267–274. https://doi.org/10.1080/19768354.2010.525830

SUPPORTING INFORMATION

Additional supporting information may be found online in the Supporting Information section.

How to cite this article: Yoon J, Rhee K. Whole-body heat exposure causes developmental stage-specific apoptosis of male germ cells. *Mol Reprod Dev*. 2020;87:680–691. https://doi.org/10.1002/mrd.23348